tainty in either method, and keeping in mind that the two methods are based on different phenomena, the discrepancy of 35% in the two results is remarkably small. In addition to J, the magnetic field studies give values for $^{ac}k_{so}$. The best value of 1.2×10^7 s^{-1} is not much different from the one used in the EPR simulations which, as pointed out above, are not very sensitive to this value. The extrapolated lifetimes for these biradicals are in general agreement with those obtained from other methods.[25] The computations also contain a number for k_{en}, listed in Table IV, which is close to the values used in the EPR simulations.

The separation of $^{ac}k_{so}$ from spin-dependent processes has therefore been achieved by the magnetic field dependent flash photolysis. The extremely small field effect observed for the C_8 acyl-alkyl biradicals shows that $^{ac}k_{so}$ predominates over spin-dependent processes for shorter chain lengths. However, the longer chain lengths show substantial field effects. If $^{ac}k_{so}$ is assumed to be independent of chain length, then this must be attributed to better singlet-triplet mixing due to a diminished J value. On the other hand, it is not clear that $^{ac}k_{so}$ is indeed independent of chain length, and the observed trend may well be due to variations in both mechanisms.

Summary

In conclusion it can be stated that a consistent picture has been developed for the kinetics of polymethylene biradicals, which are strongly dependent on both spin and chain dynamics. To unravel the importance of the various exit channels, it was found necessary to employ a broad spectrum of experimental techniques coupled with extensive computations. Theory had matched experiment quite well in most cases, and where it does not there are reasonable explanations. Much has been learned in this work regarding the mechanism of the spin-spin coupling in flexible biradicals and its overall role in the kinetics. Further work is necessary in order to fully understand the temperature dependence of the couplings by either through-bond or through-space mechanisms, and this is now an active part of our research program.

Acknowledgment. The authors thank J. A. Nairn and C. L. Braun for kindly supplying a copy of their Monte Carlo simulation program. M.D.E.F. thanks J. R. Norris for many helpful discussions on the theory of chemically induced electron spin polarization. The support of the National Science Foundation throughout the course of this work is gratefully acknowledged.

A Molecular Merry-Go-Round: Motion of the Large Macrocyclic Molecule 18-Crown-6 in Its Solid Complexes Studied by ^{2}H NMR†

C. I. Ratcliffe,*,‡ J. A. Ripmeester,‡ G. W. Buchanan,§ and J. K. Denike§

Contribution from the Steacie Institute for Molecular Sciences, National Research Council of Canada, Ottawa, Ontario, Canada K1A 0R9, and Ottawa-Carleton Chemistry Institute, Carleton University, Ottawa, Ontario, Canada K1S 5B6. *Received October 7, 1991*

Abstract: ^{2}H NMR line shape measurements were used to confirm and refine a model to account for large-amplitude motions in solid 18-crown-6 complexes previously identified from ^{13}C and ^{1}H NMR results. Reminiscent of the motion of a merry-go-round, the motion is a combined rotation and conformational adjustment of the macrocycle, in which individual $-OCH_2CH_2-$ units jump to adjacent sites in the crystal. Specifically, for the malononitrile complex, 18-crown-6·$2CH_2(CN)_2$, jump rates were obtained by modeling the intermediate-rate line shapes, yielding an activation energy of 47.6 ± 0.8 kJ/mol. Because the motion does not introduce disorder, it is diffraction invisible.

Introduction

Complexes of crown ethers and their derivatives are widely recognized as model systems for molecular recognition. The conformation of the crowns can adapt for optimum complexation of the guest. 18-Crown-6 is the archetypal macrocyclic ether, and calculations on the isolated molecule show that it is very flexible with a large number of possible conformations having only slightly different energies.[1-3] In solution the molecule rapidly interchanges among many conformations,[4] and only a single ^{13}C or ^{1}H NMR signal is observed down to 143 K.[5] In solid 18-crown-6 and its complexes, however, the molecule is usually locked into one of just a few conformations. In the ideal case where all bond angles in the crown are taken as tetrahedral, the C atoms and C-H bonds can be placed on a "diamond lattice",[1] Figure 1. The most stable conformation has D_{3d} symmetry, and the next most stable has C_i. We will refer to the latter as C_i' since many of the other conformations also have C_i symmetry. Both D_{3d} and C_i' are commonly found in solid complexes, though of course in the real world there are usually deviations from tetrahedral angles and the strict symmetry, so that only a pseudo-D_{3d} conformation is observed.

In our recent studies of the ^{13}C cross-polarization/magic angle spinning (CP/MAS) NMR of a number of molecular complexes of 18-crown-6, we found evidence that the macrocycle undergoes some kind of large-amplitude motion in the neighborhood of room temperature;[6-8] namely, (a) the coalescence of any multiple-line structure in the ^{13}C CP/MAS crown ether resonance and (b) the observation that the ^{13}C CP/MAS signal from the crown ether went through a fade-out region over a range of temperatures specific to each complex. The fade-out occurs because of interference between the coherent averaging of the ^{1}H decoupling field and the incoherent averaging due to motion of the molecule.[9] This motion was also confirmed by the narrowing of ^{1}H NMR line

† NRCC No. 33277.
‡ National Research Council of Canada.
§ Carleton University.

(1) Uiterwijk, J. W. H. M.; Harkema, S.; van de Waal, B. W.; Gobel, F.; Nibbeling, H. T. M. *J. Chem. Soc., Perkin Trans. 2* **1983**, 1843.
(2) Uiterwijk, J. W. H. M.; Harkema, S.; Feil, D. *J. Chem. Soc., Perkin Trans. 2* **1987**, 721.
(3) Billeter, M.; Howard, A. E.; Kuntz, I. D.; Kollman, P. A. *J. Am. Chem. Soc.* **1988**, *110*, 8385.
(4) Straatsma, T. P.; McCammon, J. A. *J. Chem. Phys.* **1989**, *91*, 3631.
(5) Dale, J.; Kristiansen, P. O. *J. Chem. Soc., Chem. Commun.* **1971**, 670.
(6) Buchanan, G. W.; Morat, C.; Ratcliffe, C. I.; Ripmeester, J. A. *J. Chem. Soc., Chem. Commun.* **1989**, 1306.
(7) Buchanan, G. W.; Kirby, R. A.; Ripmeester, J. A.; Ratcliffe, C. I. *Tetrahedron Lett.* **1987**, *28*, 4783.
(8) Watson, K. A.; Fortier, S.; Murchie, M. P.; Bovenkamp, J. W.; Rodrigue, A.; Buchanan, G. W.; Ratcliffe, C. I. *Can. J. Chem.* **1990**, *68*, 1201.
(9) Rothwell, W. P.; Waugh, J. S. *J. Chem. Phys.* **1981**, *74*, 2721.

0002-7863/92/1514-3294$03.00/0 Published 1992 by the American Chemical Society

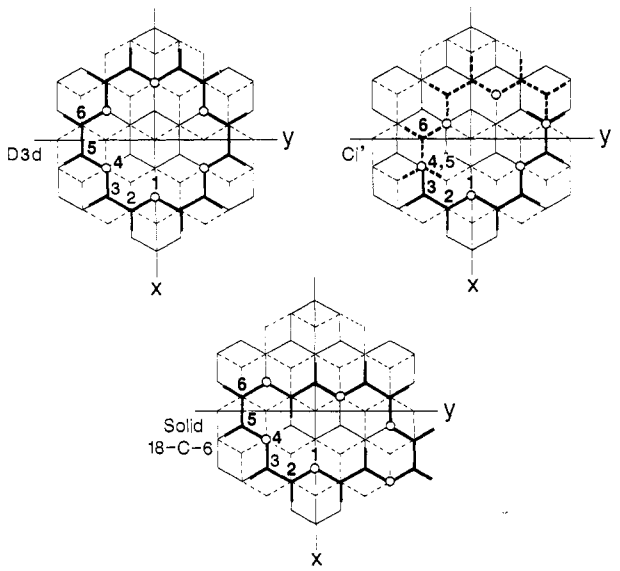

Figure 1. Representations of the D_{3d}, C_i', and solid 18-crown-6 conformations on the grid of the "diamond lattice". Solid lines represent bonds of the macrocycle on the "zero" grid, and dashed lines represent bonds on the first grid above. Connections between the grids are made by vertical bonds (parallel to the z axis). The atom numbering scheme begins with an oxygen on the x axis.

shapes as the temperature increased. Although a model was postulated to describe this motion, more evidence was required to confirm the details and to derive reliable motional parameters. ^{2}H NMR is ideally suited to this end provided complexes exist in which motionally averaged line shapes are observable below their respective melting points. Consequently the malononitrile (2:1) pseudo-D_{3d},[10] benzenesulfonamide (2:1) C_i',[11] and urea (5:1) C_i'[12] complexes were selected for study on the basis of their known melting points and structures as well as activation energies estimated from the ^{13}C NMR work. Noncomplexed 18-crown-6-d_4 was also studied before the complexes were prepared since this crystallizes in yet another conformation.[13,14]

Experimental Section

The previously unknown 18-crown-6-d_4 was prepared via reaction of triethylene glycol-d_4 with the commercially available (Aldrich) 1,8-dichloro-3,6-dioxaoctane. The following procedures were employed.

Triethylene Glycol-d_4, $HO(CH_2CH_2O)_2CD_2CD_2OH$ (1). The method was adapted from that reported for the unlabeled material.[15] A 100-mL three-neck round-bottom flask equipped with a dry ice condenser, a magnetic stirrer, and a septum gas inlet was charged with diethylene glycol (22.07 g, 0.208 mol) and pulverized KOH (1.00 g, 0.018 mol). To this was added, via the septum, gaseous ethylene oxide-d_4 (MSD isotopes) (5.0 g, 0.104 mol) at room temperature while the mixture was being stirred. Stirring was continued at ambient temperature for 1 h. Subsequently, the mixture was slowly heated to 50 °C and stirred for 6 h. Following cooling to room temperature, the mixture was neutralized with 3 N HCl and slowly distilled at reduced pressure on a spinning-band column. To maximize recovery of the desired product, 10 mL of the higher boiling tetraethylene glycol was added to the crude product prior to the spinning-band distillation. The yield of triethylene glycol-d_4, bp 120–125 °C (0.4 mmHg), was 9.0 g (56%): mass spectrum (CI), M + 1, 155.0.

18-Crown-6-d_4. Again the method was adapted from that used for the unlabeled material.[16] A 250-mL three-neck round-bottom flask equipped with a magnetic stirrer, a reflux condenser, and an addition funnel was charged with **1** (9.0 g, 54.8 mmol) and 60 mL of THF. An aqueous solution of KOH (7 mL of a 60% solution) was added, and the mixture was stirred for 15 min, after which time it had darkened considerably. Subsequently, 1,8-dichloro-3,6-dioxaoctane (10.9 g, 58.4 mmol) in 10 mL of THF was added over a 5-min period. The resulting solution was stirred vigorously and refluxed for 24 h. Following cooling and solvent removal at reduced pressure, the resulting thick brown slurry was diluted with dichloromethane (50 mL) and filtered to remove insoluble salts. These salts were washed with dichloromethane (3 × 25 mL), and the combined organics were dried over sodium sulfate. Following solvent removal, the crude product was distilled under reduced pressure (0.1 mmHg) and all fractions with bp 130–200 °C were combined. This material (8.5 g) was stirred in the presence of acetonitrile and heated to dissolve all solids. Cooling generated crystals of the 18-crown-6-d_4–acetonitrile complex, which were collected by filtration. Subsequent dissolution of this complex in 30 mL of dichloromethane and solvent removal at reduced pressure (15 mmHg) up to 70 °C yielded, as residue, pure 18-crown-6-d_4 (3.72 g, 24%), which solidified upon cooling, mp 38–39 °C (reported 39–40 °C):[16] mass spectrum (CI), (M + 1) 268.9. The final material thus produced contained one CD_2CD_2 unit.

The three molecular complexes were prepared from 18-crown-6-d_4 as previously described.[10-12]

^{2}H NMR powder spectra were recorded on a Bruker CXP-180 spectrometer at 27.63 MHz at various temperatures by using a variable-temperature N_2 gas-flow probe with a Bruker B-VT-1000 temperature controller. A phase alternated quadrupole echo pulse sequence[17] was used with a delay time of 35 μs between X and Y pulses of 2.6–3.0 μs.

Model

The model tentatively suggested in ref 6 was born of the necessity of accommodating a large-amplitude motion (NMR results) while at the same time preserving well-defined atomic coordinates (X-ray structures). For all conformations (D_{3d}, C_i', etc., see Figure 1) this can be accomplished if the whole macrocycle rotates such that each $-OCH_2CH_2-$ unit moves to an adjacent site, simultaneously adjusting its conformation to match the site it enters (i.e., the conformation at any particular crystallographic site is always the same). For a true D_{3d} case this would correspond to reorientation between adjacent sites 60° apart. For D_{3d}, however, reorientation could conceivably also occur between sites 120° apart without the need for conformational adjustment.

^{2}H NMR studies can provide very specific information about the motion of the C–D bonds, i.e., direct evidence which can either confirm or refute this model. All the necessary theory of ^{2}H NMR and the effects of molecular motion have been described in detail elsewhere,[18-23] but it will be useful to discuss briefly some of the salient features of ^{2}H NMR powder line shapes. ^{2}H ($I = 1$) NMR in solids is generally dominated by the quadrupole coupling tensor (arising from the interaction of the nuclear quadrupole with the electric field gradient (efg) tensor) which acts as the major perturbation on the Zeeman interaction. A specific orientation of the quadrupole coupling tensor with respect to the field produces a two-line spectrum symmetric about the Zeeman frequency. The powder line shape then results from the summation of such line pairs for a distribution over all orientations. They show either two or three pairs of characteristic features (edges, shoulders, and peaks) separated by frequencies

$$\begin{aligned} \Delta\nu_{zz} &= 3\chi/2 \\ \Delta\nu_{yy} &= 3\chi(1+\eta)/4 \\ \Delta\nu_{xx} &= 3\chi(1-\eta)/4 \end{aligned} \qquad (1)$$

where the quadrupole coupling constant is $\chi = e^2qQ/h$ in hertz and the asymmetry parameter is $\eta = (\Delta\nu_{yy} - \Delta\nu_{xx})/\Delta\nu_{zz}$. In the

(10) Kaufmann, R.; Knochel, A.; Kopf, J.; Oehler, J.; Rudolph, G. *Chem. Ber.* **1977**, *110*, 2249.
(11) Knochel, A.; Kopf, J.; Oehler, J.; Rudolph, G. *J. Chem. Soc., Chem. Commun.* **1978**, 595.
(12) Harkema, S.; van Hummel, G. J.; Daasvatn, K.; Reinhoudt, D. N. *J. Chem. Soc., Chem. Commun.* **1981**, 368.
(13) Dunitz, J. D.; Seiler, P. *Acta Crystallogr.* **1974**, *B30*, 2739.
(14) Maverick, E.; Seiler, P.; Schweizer, W. B.; Dunitz, J. D. *Acta Crystallogr.* **1980**, *B36*, 615.
(15) Matignon, C.; Moreau, H.; Dode, M. *Bull. Soc. Chim. Fr.* **1934**, *5*, 1308.
(16) Gokel, G. W.; Cram, D. J.; Liotta, C. L.; Harris, H. P.; Cook, F. L. *J. Org. Chem.* **1974**, *39*, 2445.
(17) Davis, J. H.; Jeffrey, K. R.; Bloom, M.; Valic, M. I.; Higgs, T. P. *Chem. Phys. Lett.* **1976**, *42*, 390.
(18) Barnes, R. G. In *Advances in Nuclear Quadrupole Resonance*; Smith, J. A. S., Ed.; Heyden: London, 1974; Vol. 1, p 335.
(19) Wittebort, R. J.; Olejniczak, E. T.; Griffin, R. G. *J. Chem. Phys.* **1987**, *86*, 5411.
(20) Greenfield, M. S.; Ronemus, A. D.; Vold, R. L.; Vold, R. R.; Ellis, P. D.; Raidy, T. E. *J. Magn. Reson.* **1987**, *72*, 89.
(21) Spiess, H. W.; Sillescu, H. *J. Magn. Reson.* **1981**, *42*, 381.
(22) Vega, A. J.; Luz, J. *J. Chem. Phys.* **1987**, *86*, 1803.
(23) Ratcliffe, C. I. *J. Phys. Chem.* **1987**, *91*, 6464.

Table I. Euler Angles for the Various Sets of Six Exchanging C–D Sites

	set 1				set 2			
	C[a] atom	α	β	γ	C atom	α	β	γ
D_{3d}	2	0	0	0	3	0	(180 + Td)	60
	5	0	(180 + Td)	60	6	0	0	120
	8	0	0	120	9	0	(180 + Td)	180
	11	0	(180 + Td)	180	12	0	0	240
	14	0	0	240	15	0	(180 + Td)	300
	17	0	(180 + Td)	300	18	0	0	0
C_i'	2	0	0	0			as above	
	5	120	(180 + Td)	300				
	8	0	0	120				
	11	0	(180 + Td)	180				
	14	300	(360 − Td)	240				
	17	0	(180 + Td)	300				
solid 18-C-6	2	0	0	0			as above	
	5	0	(180 + Td)	60				
	8	0	Td	180				
	11	0	(180 + Td)	180				
	14	0	0	240				
	17	0	180	0				

[a] Atom numbering scheme as in Figure 1.

so-called axial case $\eta = 0$ and $\Delta\nu_{xx} = \Delta\nu_{yy} = \Delta\nu_{zz}/2$. The $\Delta\nu_{ii}$ are proportional to the principal axis components of the effective quadrupole coupling tensor or efg tensor, but information regarding signs of these is lost.

Molecular motion at sufficiently high rates can cause changes in the ^{2}H NMR line shape. Differing degrees of line shape averaging are observed, depending on the rate of reorientation and the orientations of the principal axes of the efg tensor relative to the rotation axis. In the fast-motion limit (reorientation rates about 10^7 jumps/s or faster), analytical expressions for the line shapes are relatively easy to obtain:[19,20,23] The orientation of the tensor must first be described in a final reference frame in terms of the Euler angles

$$\mathbf{V}(\alpha, \beta, \gamma) = \mathbf{R}\mathbf{V}_{pas}\mathbf{R}^{-1} \quad (2)$$

where $\mathbf{R}$ is the Euler angle rotation matrix describing the coordinate transformation and $\mathbf{V}_{pas}$ is the tensor in its principal axis system. The fast-motion line shape is then given by an effective tensor which is the population weighted average of the tensor components in the final frame for all the sites (orientations) visited during the motion:

$$\mathbf{V}_{eff} = \sum_{i=1,n} \mathbf{V}_i(\alpha, \beta, \gamma)\mathbf{p}_i / \sum_{i=1,n} \mathbf{p}_i \quad (3)$$

where $\mathbf{p}_i$ is the population factor of site i.

Intermediate-rate line shapes depend on the specific rate of motion and the experimental details (e.g., on the echo delay time) and have to be calculated numerically. Methods for doing this are well established.[19-22]

As a starting point we will consider idealized "diamond lattice" 18-crown-6 molecules where all bond angles are taken as tetrahedral, for the D_{3d}, C_i', and solid 18-crown-6 conformations. Reference frames were chosen in a similar way for each conformation as indicated in Figure 1, such that the Z axis is parallel to one of the 3-fold axes of the diamond lattice (hence perpendicular to the molecular plane in the D_{3d} and solid 18-crown-6 conformations) and such that the X axis passes through an O atom, which becomes O1 in the numbering scheme.

In the case of C–D bonds it is generally a good approximation to place the principal ZZ axis of the efg tensor along the bond vector, and we can make a reasonable assumption that the YY or XX component of the tensor will be perpendicular to the CD_2 plane. One can then proceed to define the Euler angles necessary to rotate from the principal axis system of the tensor for each C–D bond to the reference frame. These are given in Table I grouped in sets corresponding to the six sites which would be visited by a particular deuteron. There can be no exchange between the four sites within each of the six $-OCH_2CH_2-$ units, and hence there are four sets of six interchangeable deuteron positions. Furthermore the three conformations considered here all have a center of symmetry, so these four sets fall into pairs of equivalent sets.

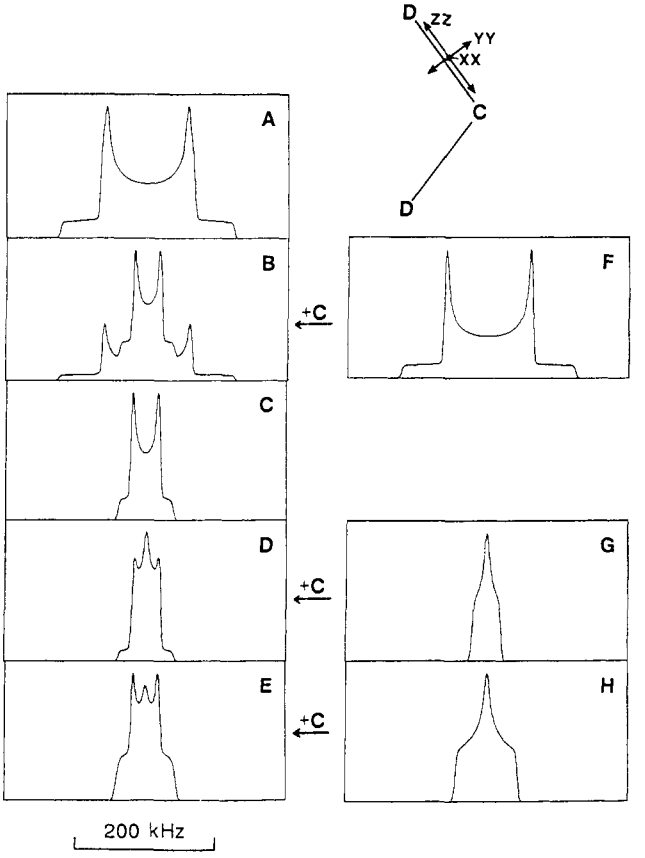

Figure 2. Calculated static and fast-motion-limit ^{2}H NMR line shapes. Parameters are given in Table II. A, static; B, 3-fold reorientation of D_{3d} conformation; C, six-site exchange of D_{3d}; D, six-site exchange of C_i'; E, six-site exchange for solid 18-crown-6. B, D, and E are 1:1 composite line shapes of C with F, G, and H, respectively. The simulated spectra were convolved with a Gaussian broadening function of half-width 5 kHz. The orientation of the static efg tensor with respect to the C–D bond is shown at the top right.

Assuming values for the static tensor components derived from the low-temperature spectrum of the malononitrile complex, the effective tensors averaged over six sites can then be calculated for each of the sets in Table I. A priori it is not known whether the static XX or YY tensor component is perpendicular to the CD_2 plane, but the two alternatives do give different averaged tensors. It was found that if the smallest component XX is chosen to be perpendicular to the CD_2 plane, much better agreement with the observed fast motion limit line shape was obtained. This tensor orientation is indicated in the inset of Figure 2. In the set 1 cases of C_i' and solid 18-crown-6, the averaged tensors were not diagonal in the chosen reference frame. In the special case of 3-fold reorientation of the D_{3d} molecule, the exchanging sites must be subdivided into sets of three, of which there are two distinct types: (a) those with C–D parallel to the rotation axis ($\beta = 0$) and (b) those with C–D at an angle of $\beta = (180 + \text{Td})$. The resulting averaged spectral parameters are given in Table II and the corresponding line shapes in Figure 2. Clearly in most cases the two sets of sites average differently, which gives rise to the composite line shapes B, D, and E in Figure 2. For the six-site D_{3d} case, sets 1 and 2 average identically to give line shape C, which is one component of all the other cases. Three-fold reorientation of the D_{3d} conformation produces the very distinct line shape B. In all the other cases the line shapes are considerably narrowed.

Results and Discussion

The ^{2}H NMR line shape of noncomplexed solid 18-crown-6-d_4 at ambient temperature, Figure 3, appears to be unaveraged by motion with $\chi = 157.6$ kHz and $\eta = 0.0661$. However, the

Table II. Calculated Fast Motion Limit Line Shape Components for the Diamond-Lattice Conformations

	spectrum, Figure 2	$\Delta\nu_{zz}$[a]	$\Delta\nu_{yy}$[a]	$\Delta\nu_{xx}$[a]	χ[a]	η
static[b]	A	246.1	131.8	114.3	164.1	0.0711
3-fold D_{3d}: C + F → B	F	246.1	123.05	123.05	164.1	0.0
6-site D_{3d}	C	78.14	39.07	39.07	52.1	0.0
6-site C_i': C + G → D	G	39.18	39.18	0.0	26.1	1.0
6-site solid 18-C-6: C + H → E	H	88.56	86.23	2.33	59.0	0.9474

[a] In kilohertz. [b] Calculations based on static line shape components observed for the malononitrile complex.

Table III. Observed Line Shape Components for the 18-Crown-6-d_4·2$CH_2(CN)_2$ Complex Compared with Calculated Values

	$\Delta\nu_{zz}$[a]	$\Delta\nu_{yy}$[a]	$\Delta\nu_{xx}$[a]	χ[a]	η
static	246.1	131.8	114.3	164.1	0.0711
6-site D_{3d} diamond lattice, calcd	78.14	39.07	39.07	52.1	0.0
obsd 373 K	69.6	34.8	34.8	46.4	0.0
adjusted angle calcn[b]	69.04	34.52	34.52	46.03	0.0

[a] In kilohertz. [b] Euler β = 0° becomes 5.71°, β = (180 + Td) = 289.47° becomes 285.66°.

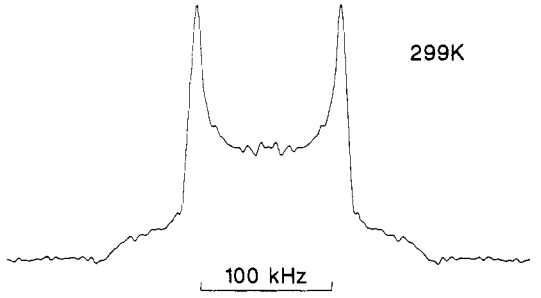

Figure 3. ^2H NMR line shape of solid 18-crown-6-d_4 at 299 K.

observation that the intensity was rather low might be an indication that the line shape is just beginning to show the effects of motional averaging (jump rate about 10^3–10^4 Hz). Since the solid melts at about 312 K, no further temperatures were investigated.

For 18-crown-6·2$CH_2(CN)_2$, a pseudo-D_{3d} case, however, fast motion limit line shapes are clearly obtained by 350 K, Figure 4. From the static line shape, which is observed below ~220 K, the intermediate line shapes undergo pronounced changes in shape and intensity, narrowing to a single sharp line at room temperature, but then broadening again and finally giving an axially symmetric line in the fast-motion limit above 350 K. The 373 K line shape shows that all the deuterons are behaving in a similar manner, ruling out the three-site D_{3d} model but matching the prediction of the six-site D_{3d} model. However, the 373 K line is significantly narrower than predicted from the diamond-lattice model (see Table III). This should not be surprising, considering the distortions from the ideal symmetry. In fact, from the information given in the crystallographic study[10] one can calculate that, on average, the C–D bonds are tilted off the diamond-lattice bond axes by about 6° for the axial bonds and by about 4° for the equatorial bonds. Recalculating the averaged line shape with these adjustments in the β Euler angles then produces an almost perfect match (Table III).

This is almost too good to be true, but further confirmation of the essential correctness of the model comes from a simulation of the intermediate-rate line shapes. The calculations were performed using a considerably modified version of the program of Vega and Luz.[22] A jump matrix was constructed for jumps between adjacent sites, and the adjusted β angles were used. Calculated line shapes are shown in Figure 5. The comparison between simulation and experiment is again remarkable. Observed

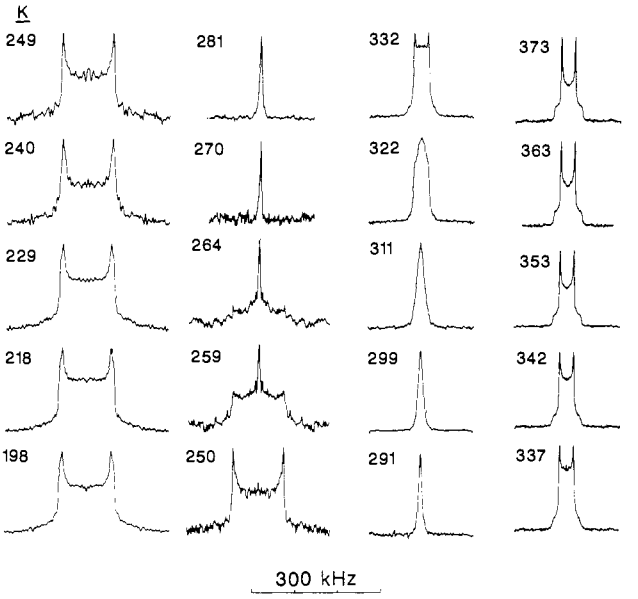

Figure 4. ^2H NMR line shapes of 18-crown-6-d_4·2$CH_2(CN)_2$ as a function of temperature.

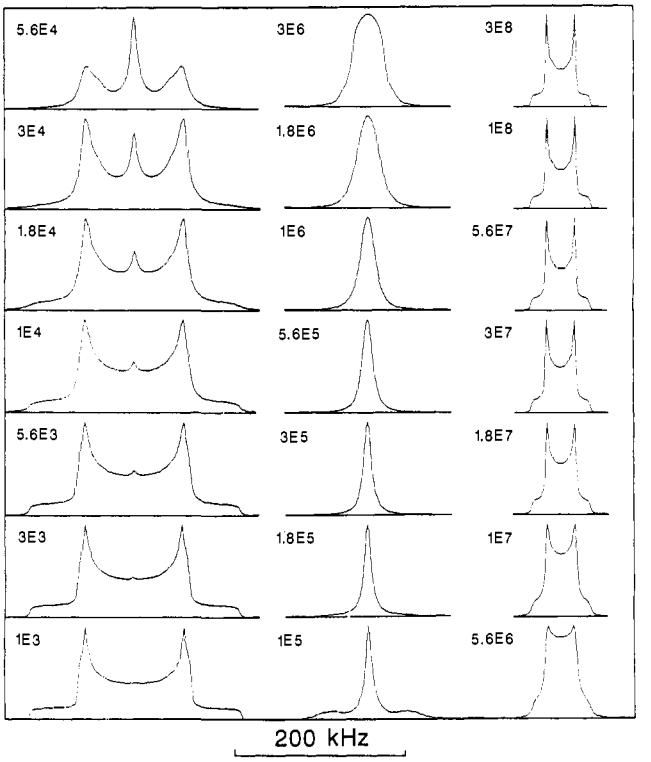

Figure 5. Simulated ^2H NMR line shapes for 18-crown-6·2$CH_2(CN)_2$ as a function of jump rate to adjacent $-OCH_2CH_2-$ sites.

and calculated line shapes were matched, allowing a correlation of jump rate with temperature, from which an Arrhenius plot (Figure 6) gives an activation energy E_a for the motion. An additional point can be obtained for the temperature at which the echo amplitude is a minimum. A linear least-squares fit gave E_a = 47.6 ± 0.8 kJ/mol (correlation coefficient R = 0.9986). The rough estimate obtained from the ^{13}C CP/MAS fade-out temperature was about 39 kJ/mol.[6]

The unusual narrowing and rebroadening of the line is reminiscent of the behavior of the ^2H NMR spectra of cyclohexane C_6D_{12} in a clathrate related to the Hofmann-type clathrates,[24] where the cyclohexane undergoes two motions with different rates,

(24) Nishikiori, S.; Ratcliffe, C. I.; Ripmeester, J. A. *J. Phys. Chem.* **1990**, *94*, 8098.

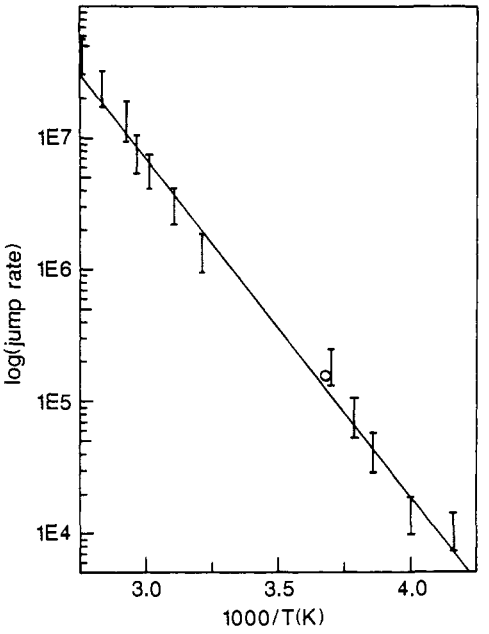

Figure 6. Arrhenius plot of jump rate versus reciprocal temperature for 18-crown-6-d_4·2$CH_2(CN)_2$ obtained by matching experimental and simulated line shapes. The point obtained for the echo intensity minimum is indicated by the circle.

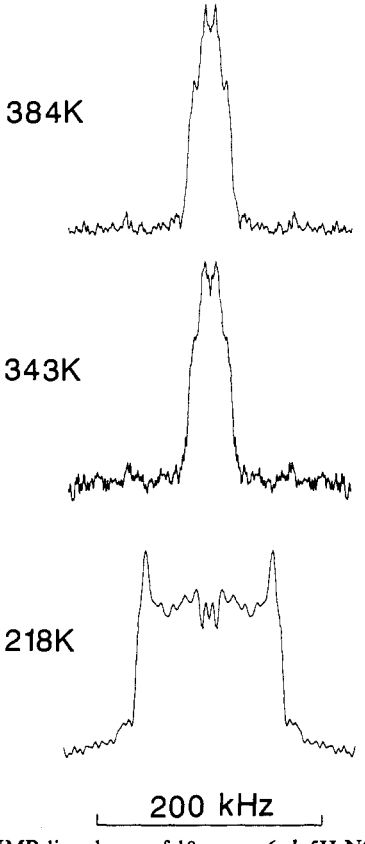

Figure 7. ^2H NMR line shapes of 18-crown-6-d_4·5H_2NCONH_2 at low and high temperatures.

i.e., an inversion motion occurs when the molecule already has rapid n-fold reorientation. In the 18-crown-6 D_{3d} situation the two motions are in effect simultaneous, but in both cases axial and equatorial deuterons exchange while the molecule reorients.

The results for two C_i' cases, complexes with urea (5:1) and benzenesulfonamide (2:1), shown in Figures 7 and 8, respectively, also show considerable narrowing before melting, to widths less than those calculated for six-site exchange. Unfortunately, detailed analysis of these line shapes is not possible for a number of reasons:

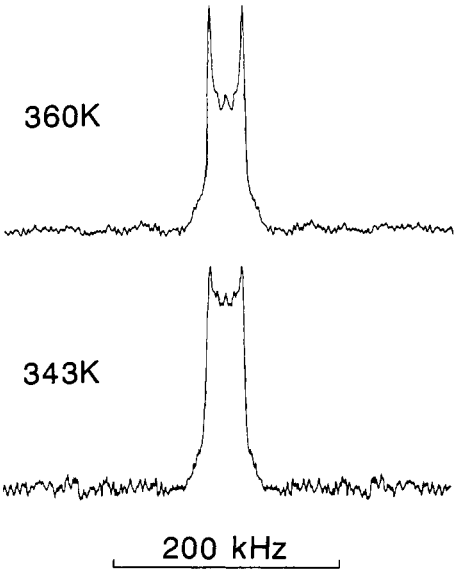

Figure 8. ^2H NMR line shapes of 18-crown-6-d_4·2$PhSO_2NH_2$.

(a) The urea complex has two inequivalent 18-crown-6 molecules,[12] both C_i', which is possibly a major complication responsible for our not being able to define tensor components from the fast-motion line shape. (b) The benzenesulfonamide complex line shape is not quite in the fast-motion limit at 360 K, indicated by a dependence of the line shapes on the quadrupole echo delay time. (c) Distortions from the ideal diamond lattice geometries are more severe in these cases. This may also account for the observed line shape not matching that predicted (D in Figure 2). (d) The assumptions about the orientations of the quadrupole coupling tensor axes may not be strictly valid for the CD_2 groups at the site of the kinks in the C_i' conformation.

Nevertheless, it would be impossible for the degree of averaging observed to be brought about by any local-site motion, so the line shapes still provide strong evidence for the reorientation of the whole macrocycle, complementary to the ^{13}C NMR evidence.[6]

In light of the low activation energies for conformational changes of the free molecule,[1-3] the activation energies for the motion in the solid complexes, some 40–50 kJ/mol, derive mainly from intermolecular contacts. The equilibrium structures therefore have individual O and CH_2 units librating in quite deep potential wells. On account of the Boltzmann factor, molecules in the process of jumping (i.e., above the barrier) at any instant represent a *very small* fraction of the total and hence do not contribute significantly to diffraction. The librational motion in the potential wells does produce some elongation of the thermal ellipsoids along the ring; compare, for example, the structures of 18-crown-6-2CH_3NO_2 (pseudo-D_{3d}) at 123 K[25] and 295 K.[26] For all purposes, therefore, the large-amplitude motion is invisible to diffraction methods.

Conclusion

The ^2H NMR line shape studies provide very strong evidence for the validity of the six-site exchange model, particularly so in the pseudo-D_{3d} case studied. As each neighboring site is visited, the CD_2 groups must bob up and down; the similarity of the motion to that of a merry-go-round is obvious. However, the analogy breaks down when one recognizes that a backward jump is just as likely as a forward jump; but that would make a very interesting ride! It is remarkable that such a large and flexible molecule is reorienting at rates of the order of 10^5–10^6 jumps/s at room temperature. 18-Crown-6 is not the first example of macrocycle rotation, however, other large-ring examples being porphine[27] and coronene,[28] but these are both rigid rings. The large-amplitude

(25) Rogers, R. D.; Richards, P. D. *J. Inclusion Phenom.* **1987**, *5*, 631.
(26) Rogers, R. D.; Green, L. M. *J. Inclusion Phenom.* **1986**, *4*, 77.
(27) Frydman, L.; Olivieri, A. C.; Diaz, L. E.; Frydman, B.; Kustanovich, I.; Vega, S. *J. Am. Chem. Soc.* **1989**, *111*, 7001.

rotation-conformational adjustment of 18-crown-6 is unique. It would be interesting to look for cases where the crown could rotate without conformational change. It would also be of interest to see if the large cyclic alkanes (which are known from ^{13}C CP/MAS studies to have mobility in the solid phase[29-31]) undergo similar kinds of motion, exchanging CH_2 groups or larger units.

Acknowledgment. G.W.B. thanks the Natural Sciences and Engineering Research Council of Canada (NSERC) for continued financial support via an operating grant.

(28) Fyfe, C. A.; Dunell, B. A.; Ripmeester, J. A. *Can. J. Chem.* **1971**, *49*, 3332.
(29) Moller, M.; Gronski, W.; Cantow, H.-J.; Hocker, H. *J. Am. Chem. Soc.* **1984**, *106*, 5093.
(30) Drotloff, H.; Emeis, D.; Waldron, R. F.; Moller, M. *Polymer* **1987**, *28*, 1200.
(31) Drotloff, H.; Rotter, H.; Emeis, D.; Moller, M. *J. Am. Chem. Soc.* **1987**, *109*, 7797.

Alkali Metal Atom Induced Acetylene-Vinylidene Rearrangement: Matrix Isolation ESR Study

Paul H. Kasai

Contribution from the IBM Almaden Research Center, 650 Harry Road, San Jose, California 95120. *Received November 4, 1991*

Abstract: Interactions between alkali metal atoms and acetylene molecules cocondensed in argon matrices were examined by ESR spectroscopy. The following are shown: (1) No reaction occurs between alkali metal atoms in the ^2S ground state and acetylene molecules, but the side-on π complexes are formed between alkali metal atoms in the ^2P excited state and the acetylene molecules. (2) Subsequent exposure of the π complex to light corresponding to the $\pi \rightarrow \pi^*$ transition in the acetylene moiety results in its isomerization to the vinylidene form $M{:}C{=}CH_2$. The **g** tensors, the proton, and the alkali metal-atom hyperfine coupling tensors of the observed π and vinylidene complexes and the ^{13}C hfc tensor of the Li-acetylene π complex were determined. In the case of the Na/acetylene/argon system, only the vinylidene complex was observed due to coincidence of the 3s $\rightarrow$ 3p transition of Na atom and the $\pi \rightarrow \pi^*$ transition of the π complex.

Introduction

The acetylene-vinylidene isomerization process has been the subject of many theoretical studies.[1] It is now reasonably well agreed that vinylidene, the simplest form of carbene $H_2C{=}C{:}$, exists as a bound molecule. The ground state of vinylidene lies ~44 kcal/mol above that of acetylene, however, and the barrier for the vinylidene-to-acetylene rearrangement is only 2-4 kcal/mol. The situation for the corresponding anionic system differs significantly. The isomerization process between the acetylene anion and vinylidene anion has been shown to be thermoneutral; a barrier of 40 ~ 50 kcal/mol has been computed for the rearrangement, however.[2,3] Experimental values determined by Ervin, et al.,[4] based on the photoelectron spectroscopy of vinylidene anions, are in excellent accord with these theoretical predictions.

The effect of interacting alkali metal atoms on the acetylene-vinylidene rearrangement has also been examined theoretically.[3,5,6] Of the three possible equilibrium structures, **1**, **2**, and **3**, it has

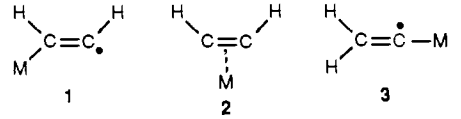

been concluded that (1) the σ-bonded structure **1** is not a bound state, (2) the π-bonded state **2** is weakly bound (by several kcal/mol), and (3) the Li-vinylidene structure **3** is also an equilibrium state; it is slightly less stable than **2** (by several kcal/mol), and there exists a high barrier (40 ~ 50 kcal/mol) against the isomerization process between the two structures.

Manceron and Andrews[7] detected, in their matrix isolation IR study, the formation of the π complex **2** between the Li atoms and acetylene molecules cocondensed in argon matrices at 15 K in total accord with the theoretical result briefed above. In structure **2** the C-H bonds are bent away from the metal atom as depicted. Based on the relative intensities of the symmetric and antisymmetric C-H stretching modes, they estimated the CCH angle of 140°, also in an excellent accord with the theoretical value (139°).[5,6] The corresponding π complexes were not observed with heavier alkali metal atoms (Na, K, Cs); these metal atoms catalyzed intermolecular hydrogen transfer within hydrogen-bonded acetylene molecules, however.[8]

We had earlier conducted an ESR study of argon matrices containing Na atoms and acetylene molecules, and observed photoinduced formation of Na-acetylene complexes.[9] The ESR spectrum of the complex was characterized by small hyperfine coupling (hfc) interaction with one ^{23}Na nucleus, and large, essentially isotropic hfc interaction with two equivalent hydrogen nuclei, and was hence assigned to the complex of the vinylidene structure **3**. The assignment appeared to be in contradiction with the theoretical results[3,5,6] reported afterward. As will be shown later, the issue was unsettled further by INDO molecular orbital calculations predicting that the isotropic components of the hfc tensors of the Na and hydrogen nuclei of the π complex **2** (with bent acetylene) would be very similar to those of the vinylidene form **3**. A thorough reexamination of the alkali metal atom-acetylene interactions by ESR thus appeared clearly in order.

We report here the result of such (re)examination of the alkali atom (Li, Na, K)-acetylene interactions in argon matrices. We

(1) Gallow, M. M.; Hamilton, T. P.; Schaefer, H. F. *J. Am. Chem. Soc.* **1990**, *112*, 8714 and references cited therein.
(2) Frenking, G. *Chem. Phys. Lett.* **1983**, *100*, 484.
(3) Sakai, S.; Morokuma, K. *J. Phys. Chem.* **1987**, *91*, 3661.
(4) Ervin, K. M.; Ho, J.; Lineberger, W. C. *J. Chem. Phys.* **1989**, *91*, 5974.
(5) Pouchan, C. *Chem. Phys.* **1987**, *111*, 87.
(6) Nguyen, M. T. *J. Phys. Chem.* **1988**, *92*, 1426.
(7) Manceron, L.; Andrews, L. *J. Am. Chem. Soc.* **1985**, *107*, 563.
(8) Manceron, L.; Andrews, L. *J. Phys. Chem.* **1985**, *89*, 4094.
(9) Kasai, P. H. *J. Phys. Chem.* **1982**, *86*, 4092.

0002-7863/92/1514-3299$03.00/0